

# Competitive Bond Homolysis and Intersystem Crossing in the Picosecond Time Regime. Photodissociation of 9-Bromo- and 9-Chlorofluorene in Cyclohexane

William M. McGowan and Edwin F. Hilinski\*

Contribution from the Department of Chemistry, The Florida State University, Tallahassee, Florida 32306-3006

Received December 20, 1994<sup>⊗</sup>

**Abstract:** Electronic absorption and fluorescence spectroscopies were used to study the picosecond time scale competition between intersystem crossing and carbon–halogen bond homolysis resulting from 266-nm excitation of 9-chloro- and 9-bromofluorene in the nonpolar solvent cyclohexane. From steady-state fluorescence spectroscopy, fluorescence quantum yields ( $\phi_f$ ) relative to fluorene (relative  $\phi_f = 1.0$ ) of 0.036, 0.046, and 0.034 were measured for 2-bromofluorene, 9-chlorofluorene, and 9-bromofluorene, respectively. Picosecond-resolved absorption spectroscopy permitted the detection of  $S_n \leftarrow S_1$  absorption of fluorene near 700 nm which decayed with a time constant of 5.1 ns. Within experimental error, the decay time of this transient absorption band agreed with an observed fluorescence decay time of 5.8 ns for fluorene, thereby providing support for the assignment of this absorption to  $S_1$  of fluorene. From transient absorption measurements, intersystem crossing of 2-bromofluorene occurred with a time constant of  $\sim 40$  ps ( $k_{isc} \cong 2.5 \times 10^{10} \text{ s}^{-1}$ ). Excitation of 9-chlorofluorene and 9-bromofluorene resulted in the appearance of absorptions assigned to the 9-fluorenyl radical and to  $T_1$  of the 9-halofluorene. Additional evidence supporting the assignments of absorptions to  $T_1$  of the 9-halofluorenes was provided from transient absorption experiments in which triplet energy transfer was used to populate  $T_1$  of fluorene, 9-chlorofluorene, and 9-bromofluorene. Carbon–halogen bond homolysis does not occur from  $T_1$  for times up to 20 ns postexcitation for these 9-halofluorenes. For 9-chloro- and 9-bromofluorene, intersystem crossing and bond homolysis depopulate  $S_1$ . Intersystem crossing in 9-bromofluorene occurs faster than in 9-chlorofluorene [ $\tau_{isc} \leq 20$  ps ( $k_{isc} \geq 5.0 \times 10^{10} \text{ s}^{-1}$ ) and  $\cong 40$  ps ( $k_{isc} \cong 2.5 \times 10^{10} \text{ s}^{-1}$ ), respectively], resulting in less 9-fluorenyl radical produced *via* bond homolysis in  $S_1$  from the bromide than from the chloride although the C–Br bond is weaker than the C–Cl bond.

## Introduction

For photodissociations of carbon–heteroatom (C–X) bonds in molecules in solution, the roles of singlet and triplet excited states have been considered in the dissociation mechanisms and in the interconversions of fragments between radical pairs and ion pairs *via* electron transfer. The photochemistry of arylmethyl derivatives and photolysis of C–X bonds have been the focus of many product and time-resolved spectroscopic studies and of several reviews.<sup>1–3</sup> However, details about the dissociative processes in the subnanosecond time regime are still lacking. Scheme 1 outlines four mechanistic extremes which have been considered for fragmentations from a singlet excited state leading to the production of the following: (1) radical pairs and ion pairs competitively;<sup>4</sup> (2) ion pairs in equilibrium or resonance<sup>5</sup> with radical pairs without the specification of which type of pair is formed first if it is an equilibrium;<sup>6–8</sup> (3) radical pairs formed first followed by electron transfer to give ion pairs under

suitably polar solvation conditions;<sup>2,9</sup> and (4) ion pairs formed first followed by electron transfer to give radical pairs under suitably nonpolar solvation conditions.<sup>10</sup> The degree to which each of these possibilities may be operative is expected to depend on the types of functional groups present in the two fragments and the reaction medium. Recently, correlations of product distributions with expectations based upon Marcus electron-transfer theory have been used to support the involvement of interfragment electron transfer.<sup>11–13</sup> Although interfragment electron transfer has been postulated for photodissociations of arylmethyl derivatives in solution, it has not yet been detected by means of time-resolved spectroscopy.

The involvement of triplet states complicates matters further. It is interesting to note that reports for photolyses of naphthylmethyl halides<sup>14</sup> and triphenylmethyl halides<sup>10</sup> have described more products derivable from radicals or more radicals generated for chlorides than for bromides although the C–Br bond is weaker than the C–Cl bond within each series.<sup>15</sup> Several steady-state quenching studies have revealed the involvement of triplet states in the photodissociations of benzyl halides<sup>16,17</sup> but not in several naphthylmethyl systems.<sup>12–14,18</sup>

<sup>⊗</sup> Abstract published in *Advance ACS Abstracts*, June 1, 1995.

(1) Cristol, S.; Bindel, T. H. *Org. Photochem.* **1983**, *6*, 327–415.

(2) Kropp, P. J. *Acc. Chem. Res.* **1984**, *17*, 131–137.

(3) Das, P. K. *Chem. Rev.* **1993**, *93*, 119–144.

(4) Zimmerman, H. E.; Sandel, V. R. *J. Am. Chem. Soc.* **1963**, *85*, 915–921.

(5) Walling, C.; Waits, H. P.; Milovanovic, J.; Pappiaonou, C. G. *J. Am. Chem. Soc.* **1970**, *92*, 4927–4932.

(6) Appleton, D. C.; Brocklehurst, B.; McKenna, J.; McKenna, J. M.; Thackeray, S.; Walley, A. R. *J. Chem. Soc., Perkin Trans. 2* **1980**, 87–90.

(7) Appleton, D. C.; Bull, D. C.; Givens, R. S.; Lillis, V.; McKenna, J.; McKenna, J. M.; Thackeray, S.; Walley, A. R. *J. Chem. Soc., Perkin Trans. 2* **1980**, 77–82.

(8) Appleton, D. C.; Bull, D. C.; Givens, R. S.; Lillis, V.; McKenna, J.; McKenna, J. M.; Thackeray, S.; Walley, A. R. *J. Chem. Soc., Chem. Commun.* **1974**, 473–474.

(9) Kropp, P. J.; Jones, T. H.; Poindexter, G. S. *J. Am. Chem. Soc.* **1973**, *95*, 5420–5421.

(10) Manring, L. E.; Peters, K. S. *J. Phys. Chem.* **1984**, *88*, 3516–3520.

(11) Pincock, J. A.; Wedge, P. J. *J. Org. Chem.* **1994**, *59*, 5587–5595.

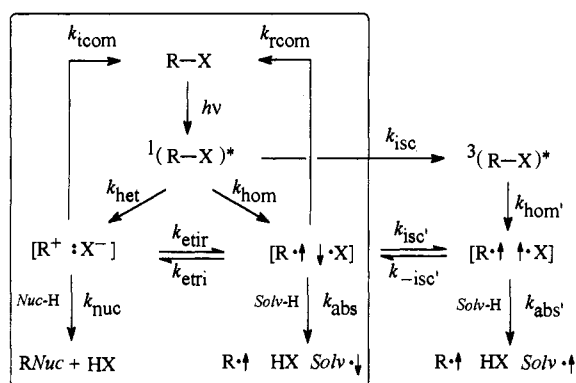
(12) Hilborn, J. W.; MacKnight, E.; Pincock, J. A.; Wedge, P. J. *J. Am. Chem. Soc.* **1994**, *116*, 3337–3346.

(13) DeCosta, D. P.; Pincock, J. A. *J. Am. Chem. Soc.* **1993**, *115*, 2180–2190.

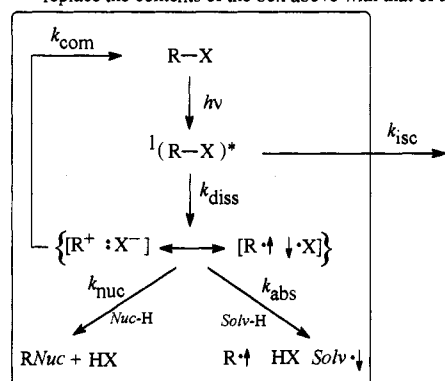
(14) Slocum, G. H.; Schuster, G. B. *J. Org. Chem.* **1984**, *49*, 2177–2185.

(15) Murov, S. L.; Carmichael, I.; Hug, G. L. *Handbook of Photochemistry*, 2nd ed.; Marcel Dekker, Inc.: New York, 1993.

## Scheme 1



If resonance instead of equilibrium exists for the ion and radical pairs, replace the contents of the box above with that of the box below.



Abbreviations for rate constants:

$k_{het}$ - bond heterolysis from singlet	$k_{icom}$ - ion pair combination
$k_{hom}$ - bond homolysis from singlet	$k_{rcom}$ - radical pair combination
$k_{isc}$ - intersystem crossing from singlet	$k_{nuc}$ - nucleophilic capture of cation
$k_{hom'}$ - bond homolysis from triplet	$k_{abs}$ - H abstraction from solvent, singlet
$k_{etir}$ - electron transfer from ions to radicals	$k_{abs'}$ - H abstraction from solvent, triplet
$k_{etri}$ - electron transfer from radicals to ions	$k_{diss}$ - bond dissociation to give ion/radical pair hybrid
$k_{isc'}$ - intersystem crossing from singlet radical pair to triplet radical pair	$k_{com}$ - pair combination in resonance hybrid
$k_{-isc}$ - intersystem crossing from triplet radical pair to singlet radical pair	

In addition to learning whether the fragments derive from within the singlet or triplet manifold, important information about the relative magnitudes of intramolecular heavy-atom effects in arylmethyl halides *vs* aryl halides will be provided from measurements of the absolute rate constants for intersystem crossing for these two types of halides. There have been no reports of time-resolved studies that address the time scales for intersystem crossing in arylmethyl halides that undergo direct photodissociation on the time scale of picoseconds. Recent results from *ab initio* CAS-MCSCF (complete active space multiconfiguration self-consistent-field) calculations<sup>19</sup> of spin-orbital coupling (SOC) revealed the enhancement of SOC in a heavy-atom containing molecule, vinyl chloride, resulting from out-of-plane deformations, particularly the C-Cl bond. The importance of out-of-plane modes in spin-orbital coupling mechanisms had been reported previously for benzene and naphthalene in the absence of heavy atoms.<sup>20</sup>

Studies on the formation of the 9-fluorenyl cation in our laboratory revealed that the singlet excited state of the precursor

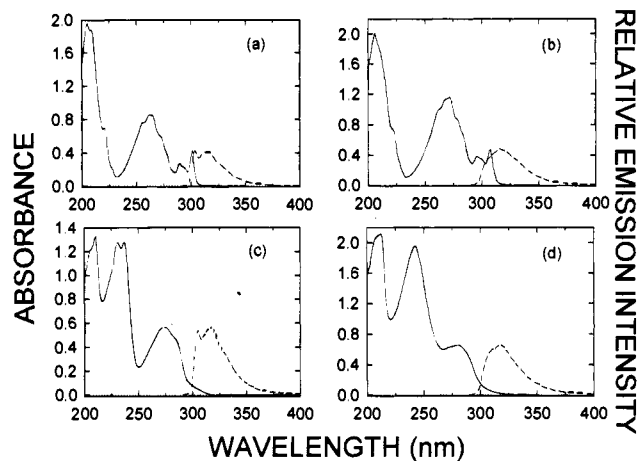
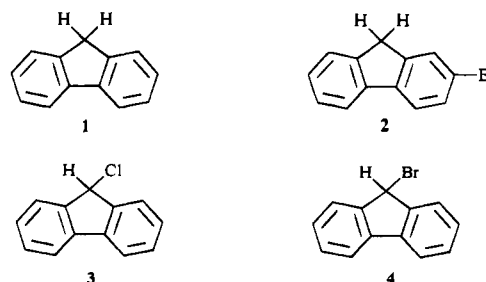


**Figure 1.** Absorption (—) and fluorescence (---) spectra recorded in cyclohexane. For fluorescence spectra,  $\lambda_{exc} = 266$  nm and a 1-cm cell were used. Specific information about sample identity, concentration, and optical path for each absorption (A) and concentration for each fluorescence spectrum (F) is as follows: (a) A, 0.20 mM fluorene and 2 mm; F, 3.0  $\mu$ M; (b) A, 0.20 mM 2-bromofluorene and 2 mm; F, 2.0  $\mu$ M; (c) A, 0.020 mM 9-chlorofluorene and 1 cm; F, 5.0  $\mu$ M; (d) A, 0.070 mM 9-bromofluorene and 1 cm; F, 8.0  $\mu$ M.

can be detected.<sup>21</sup> Picosecond<sup>21</sup> and nanosecond<sup>22</sup> time scale studies demonstrated the detectability of the triplet excited states of fluorene derivatives. In this work, we have studied photodissociations of 9-chlorofluorene and 9-bromofluorene in cyclohexane that do permit the possible detection of excited singlet and triplet states as well as the ground-state 9-fluorenyl radical resulting from the homolysis of the carbon-halogen bond. Cyclohexane was selected as the solvent to minimize the generation of 9-fluorenyl cation/halide ion pairs and to focus on the relative rates of intersystem crossing and the formation of the 9-fluorenyl radical.

## Results

**Steady-State Spectroscopy.** In this work, photophysical and photochemical comparisons are made for fluorene, 2-bromofluorene, 9-chlorofluorene, and 9-bromofluorene (1–4, respectively). Absorption and fluorescence spectra are shown in Figure 1. The fluorescence quantum yields ( $\phi_f$ ) relative to fluorene (relative  $\phi_f = 1.0$ ) are 0.036, 0.046, and 0.034 for 2-bromofluorene, 9-chlorofluorene, and 9-bromofluorene, respectively.



**Transient Absorption Spectroscopy.** Transient absorption spectra were recorded for fluorene, 9-chlorofluorene, 9-bromofluorene, and 2-bromofluorene in cyclohexane to investigate the details associated with the photodissociation of 9-halofluorenes. Sets of selected representative spectra for each of these

(16) Cristol, S. J.; Bindel, T. H. *J. Org. Chem.* **1980**, *45*, 951–957.

(17) Cristol, S. J.; Bindel, T. H. *J. Am. Chem. Soc.* **1981**, *103*, 7287–7293.

(18) Foster, B.; Gaillard, B.; Mathur, N.; Pincok, A. L.; Pincok, J. A.; Sehmbey, C. *Can. J. Chem.* **1987**, *65*, 1599–1607.

(19) Caldwell, R. A.; Jacobs, L. D.; Furlani, T. R.; Nalley, E. A.; Laboy, J. *J. Am. Chem. Soc.* **1992**, *114*, 1623–1625.

(20) Henry, B. R.; Siebrand, W. *J. Chem. Phys.* **1971**, *54*, 1072–1085.

(21) Mecklenburg, S. L.; Hilinski, E. F. *J. Am. Chem. Soc.* **1989**, *111*, 5471–5472.

(22) Gaillard, E.; Fox, M. A.; Wan, P. *J. Am. Chem. Soc.* **1989**, *111*, 2180–2186.

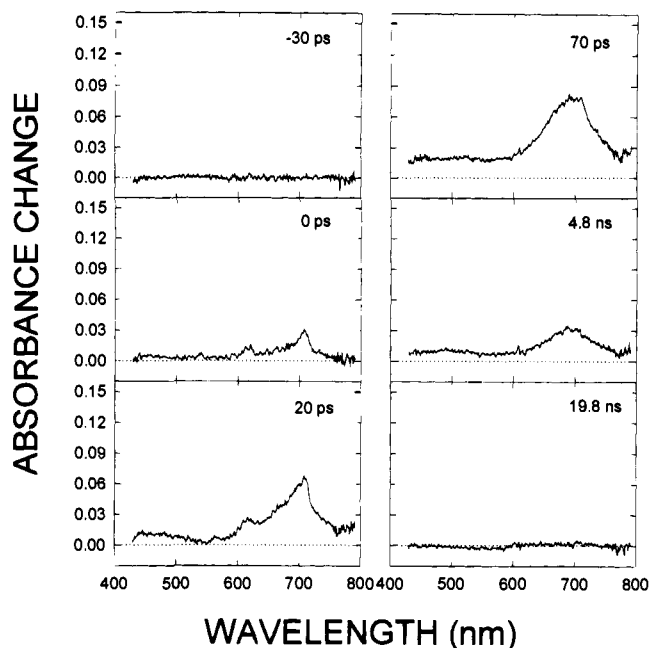


**Figure 2.** Transient absorption spectra recorded at selected times after 266-nm excitation of 0.20 mM fluorene in cyclohexane. Optical path length of flow cell = 2 mm. Delay time (average pulse energy,  $\mu\text{J}$ ): -30 ps (210); 0 ps (220); 20 ps (220); 70 ps (210); 4.8 ns (210); 19.8 ns (210).

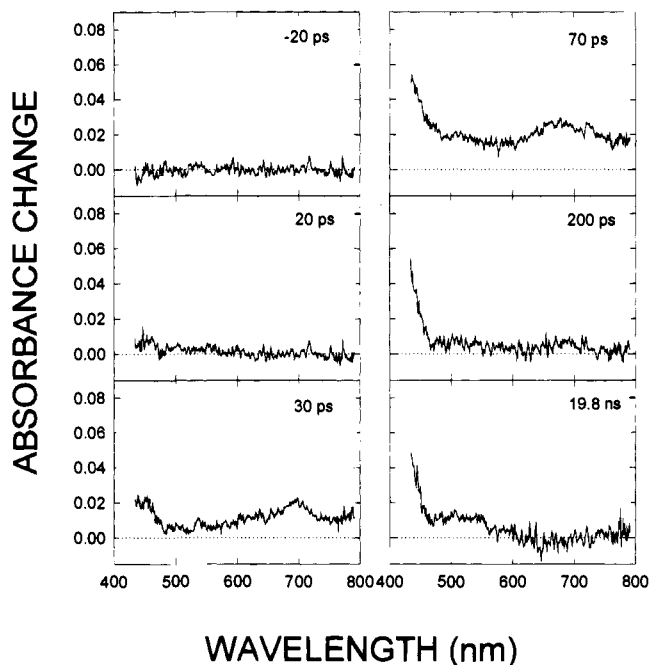


**Figure 3.** Transient absorption spectra recorded at selected times after 266-nm excitation of 0.20 mM 2-bromofluorene in cyclohexane. Optical path length of flow cell = 2 mm. Delay time (average pulse energy,  $\mu\text{J}$ ): -20 ps (210); 20 ps (210); 30 ps (200); 70 ps (220); 200 ps (200); 19.8 ns (200).

compounds are shown in Figures 2–5, respectively. Transient absorption spectra for wavelengths from approximately 420 to 790 nm were recorded for times up to 20 ns after direct excitation of these compounds in cyclohexane with 266-nm, 25-ps laser pulses. Also recorded were transient absorption spectra for cyclohexane solutions of fluorene, 9-chlorofluorene, and 9-bromofluorene in which triplet excitation energy was transferred from benzophenone that was excited with 355-nm, 25-ps pulses. Representative spectra for the triplet-sensitized

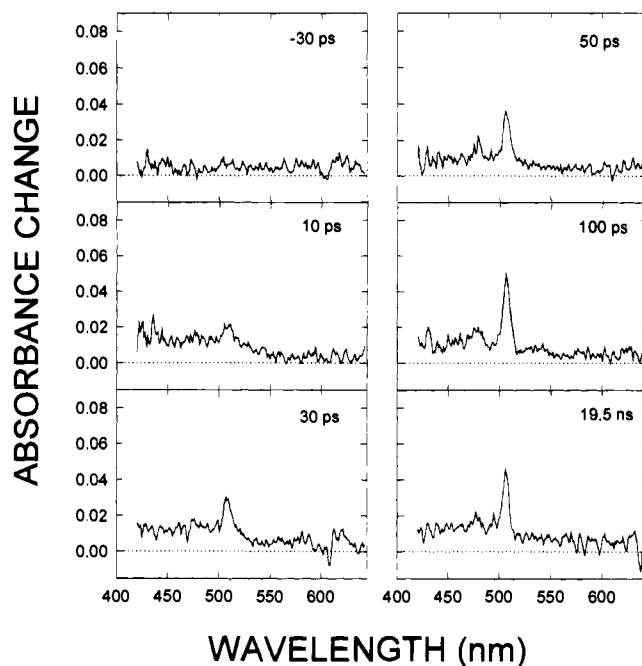


**Figure 4.** Transient absorption spectra recorded at selected times after 266-nm excitation of 0.54 mM 9-chlorofluorene in cyclohexane. Optical path length of flow cell = 2 mm. Delay time (average pulse energy,  $\mu\text{J}$ ): -30 ps (180); 10 ps (180); 30 ps (170); 50 ps (180); 100 ps (170); 19.5 ns (160).

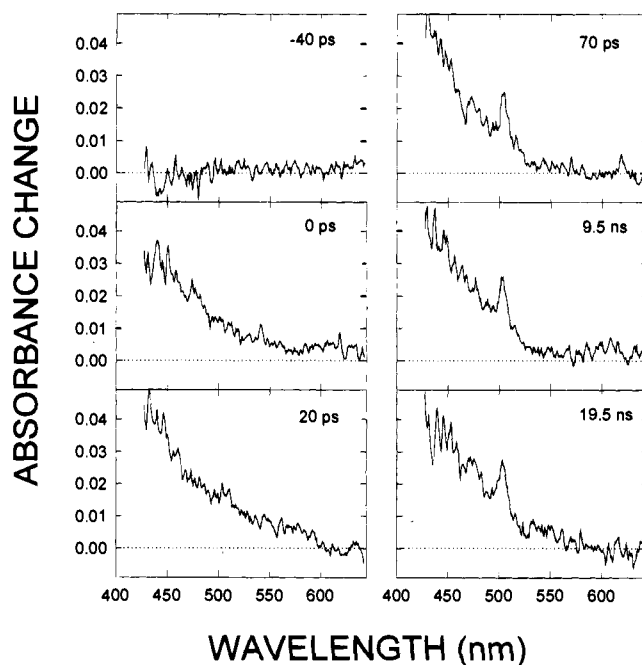


**Figure 5.** Transient absorption spectra recorded at selected times after 266-nm excitation of 0.4 mM 9-bromofluorene in cyclohexane. Optical path length of flow cell = 5 mm. Delay time (average pulse energy,  $\mu\text{J}$ ): -40 ps (161); 0 ps (149); 20 ps (150); 70 ps (145); 9.5 ns (149); 19.5 ns (153).

experiments are shown in Figures 6–8. Not all spectra that were recorded are shown in Figures 2–8.

To understand better which excited states may possibly be involved in the 9-halofluorene photohomolyses, solutions of fluorene and 2-bromofluorene in cyclohexane were studied. The transient absorption spectra recorded after direct excitation of fluorene reveal that characteristic absorption due to  $S_n \leftarrow S_1$  transitions of the fluorene chromophore appears in the 430–790-nm range probed in these experiments. At 0 ps, maxima

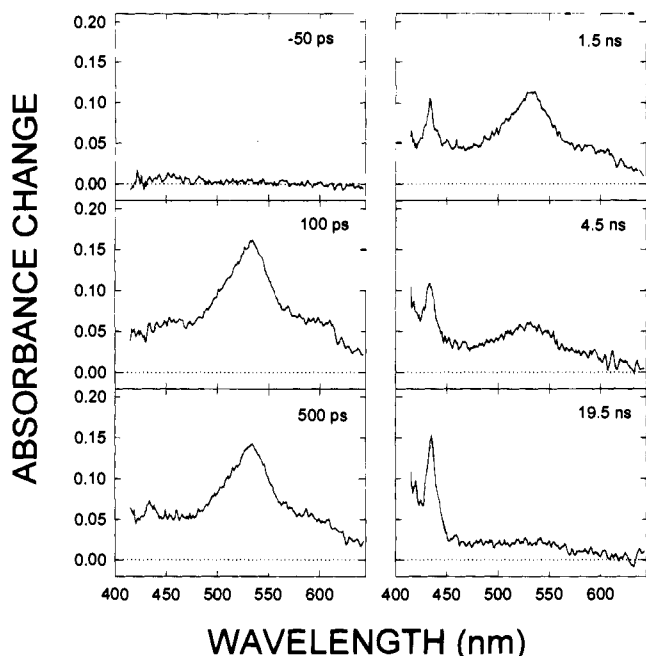


**Figure 6.** Transient absorption spectra recorded at selected times after 355-nm excitation of 50 mM benzophenone with 80 mM fluorene in cyclohexane. Optical path length of flow cell = 2 mm. Delay time (average pulse energy,  $\mu\text{J}$ ): -50 ps (145); 100 ps (145); 500 ps (145); 1.5 ns (150); 4.5 ns (150); 19.5 ns (145).

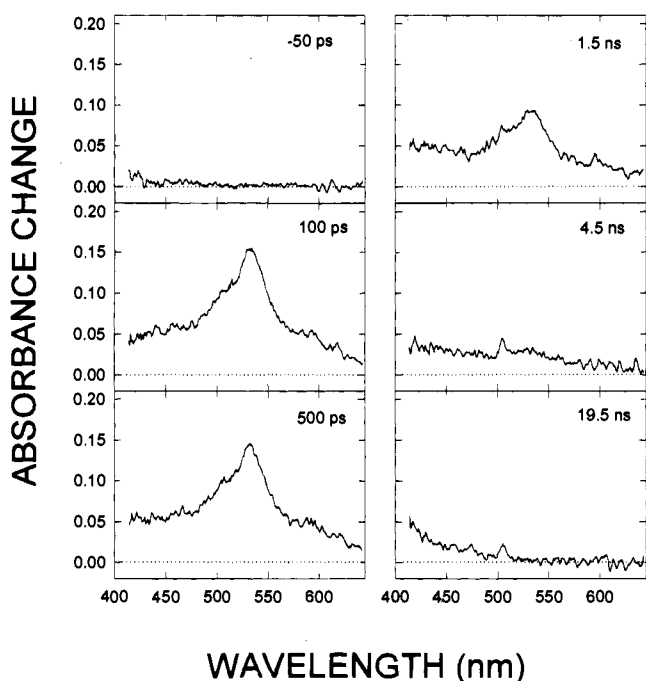


**Figure 7.** Transient absorption spectra recorded at selected times after 355-nm excitation of 50 mM benzophenone with 80 mM 9-chlorofluorene cyclohexane. Optical path length of flow cell = 2 mm. Delay time (average pulse energy,  $\mu\text{J}$ ): -50 ps (140); 100 ps (145); 500 ps (145); 1.5 ns (150); 4.5 ns (150); 19.5 ns (150).

near 620 and 715 nm are apparent and broaden as a function of time as evidenced in the spectra recorded at 10, 20, 30, and 40 ps. By 50 ps, the shape of the spectrum exhibited at longer times has broadened to that shown for 70 ps with a maximum near 700 nm which decays to base line by 19.8 ns after excitation. This decay occurred with a time constant of 5.1 ns which, as will be discussed further below, compares well with literature values of the observed fluorescence decay time.<sup>23-27</sup>

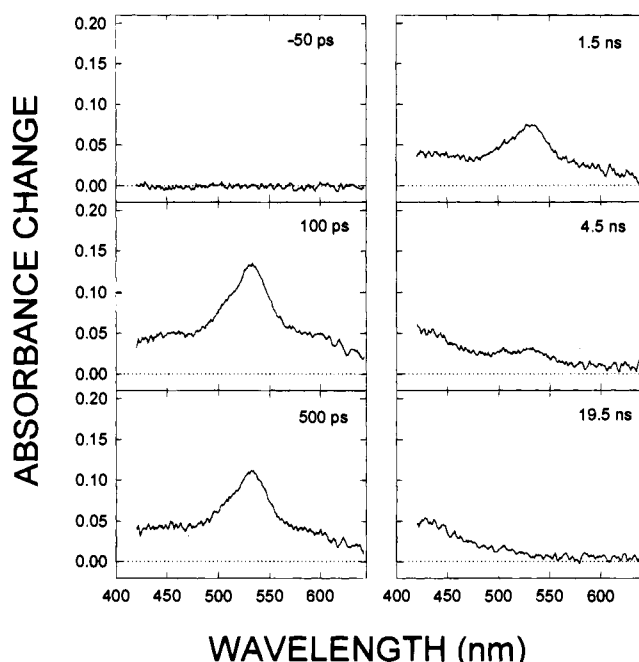


**Figure 8.** Transient absorption spectra recorded at selected times after 355-nm excitation of 50 mM benzophenone with 80 mM 9-bromofluorene cyclohexane. Optical path length of flow cell = 2 mm. Delay time (average pulse energy,  $\mu\text{J}$ ): -50 ps (170); 100 ps (175); 500 ps (170); 1.5 ns (165); 4.5 ns (165); 19.5 ns (165).

The transient absorption spectra in the 435–790-nm range recorded after direct excitation of 2-bromofluorene also exhibit a maximum near 700 nm which is assigned to  $S_n \leftarrow S_1$  transitions of the fluorene chromophore. This band decays with  $\tau \approx 40$  ps, a time constant which is much shorter than the observed lifetime of the  $S_1$  state of fluorene. A new absorption in the 435–600-nm region with a maximum at <435 nm is present at early times, grows with a time constant of  $\sim 40$  ps, and is assigned to  $T_n \leftarrow T_1$  transitions of 2-bromofluorene. This assignment is consistent with the observation, described below, of triplet–triplet absorption in the 415–600-nm region at 19.5 ns after excitation of benzophenone which transfers triplet excitation energy to fluorene and with previous reports of triplet–triplet absorption spectra for fluorene and several of its derivatives.<sup>21,22,28-33</sup>

For the direct excitation of 9-chlorofluorene, a broad absorption in the 420–550-nm range and a maximum at 505 nm were observed within the time duration of the 25-ps excitation pulse. After subtraction of the growing broad absorption in the 420–550 nm region from the maximum at 505 nm, the appearance of the 505-nm band could be fitted to a rise time of 40 ps. The broad absorption, measured at 450 nm, also exhibited a 40 ps rise time, although these data were noisier than those for the 505-nm band. Both these absorptions persist for times longer than 19.5 ns. The broad absorption is assigned to  $T_n \leftarrow T_1$

(23) Palmer, T. F.; Parmar, S. S. *J. Photochem.* **1985**, *31*, 273–288.

(24) Berlman, I. B. *J. Chem. Phys.* **1970**, *52*, 5616–5621.

(25) Berlman, I. B. *Handbook of Fluorescence Spectra of Aromatic Molecules*, 2nd ed.; Academic Press: New York, 1971.

(26) Dellonte, S.; Raffaelli, V.; Barigelletti, F. *Gazz. Chim. Ital.* **1984**, *114*, 375–378.

(27) Walden, G. L.; Winefordner, J. D. *Spectrosc. Lett.* **1980**, *13*, 793–801.

(28) Craig, D. P.; Ross, I. G. *J. Chem. Soc.* **1954**, 1589–1606.

(29) Porter, G.; Windsor, M. W. *Proc. R. Soc. London, Ser. A* **1958**, *A245*, 238.

(30) Heinzlmann, W.; Labhart, H. *Chem. Phys. Lett.* **1969**, *4*, 20–24.

(31) Alifimov, M. V.; Batekha, I. G.; Sheck, Y. B.; Gerko, V. I. *Spectrochim. Acta* **1971**, *27A*, 329–341.

(32) Bree, A.; Zwarich, R. *J. Chem. Phys.* **1969**, *51*, 903–912.

(33) Pavlopoulos, T. G. *Spectrochim. Acta* **1986**, *42a*, 1307–1310.

transitions of 9-chlorofluorene; the 505-nm band with another maximum near 480 nm is assigned to the ground-state 9-fluorenyl radical.<sup>21,22,34-36</sup> In these transient absorption spectra, no absorption due to  $S_n \leftarrow S_1$  transitions of 9-chlorofluorene is apparent.

For the direct excitation of 9-bromofluorene, a broad absorption in the 430–550-nm range and a maximum at 505 nm were observed within the time duration of the 25-ps excitation pulse. The appearances of the 505-nm band and the broad 430–550-nm absorption could be fitted to rise times of  $\leq 20$  ps, the time resolution for these particular measurements, and are assigned to the 9-fluorenyl radical and  $T_n \leftarrow T_1$  transitions of 9-bromofluorene, respectively. At times from 0 ps to 19.5 ns, no absorption due to  $S_n \leftarrow S_1$  transitions of 9-bromofluorene is apparent. The transient absorption spectra for 9-chlorofluorene and 9-bromofluorene were recorded under comparable experimental conditions. After normalization with respect to excitation pulse energy for the fixed pulse diameter at the sample, the ratios of the fluorenyl radical absorption to the broad triplet-triplet absorption are  $\sim 4:1$  and  $\sim 1:1$  for the 9-chlorofluorene and 9-bromofluorene samples, respectively.

The generation of the lowest triplet excited state of fluorene ( $E_{T_1} = 67$  kcal/mol;<sup>37</sup> 68 kcal/mol<sup>38,39</sup>) was done by means of triplet energy transfer from benzophenone ( $E_{T_1} = 69$  kcal/mol<sup>15</sup>) excited at 355 nm. Representative transient absorption spectra are shown in Figure 6. At early times such as 100 ps after excitation, the triplet-triplet absorption spectrum of benzophenone is apparent in the 415–640-nm range probed in these experiments. The absorption spectrum of triplet benzophenone decays to give the absorption spectrum of  $T_1$  of fluorene (Figure 6, 19.5 ns).

Triplet-sensitized excitation of 9-chlorofluorene was achieved via 355-nm excitation of benzophenone. The triplet-triplet absorption spectrum of benzophenone is apparent at early times, for example 100 ps in Figure 7, and decays to give a spectrum (Figure 7, 19.5 ns) which is composed of absorptions due to the 9-fluorenyl radical and  $T_1$  of 9-chlorofluorene. A weak absorption due to the radical can be seen in spectra in Figure 7 recorded at  $\geq 1.5$  ns postexcitation.

Triplet-sensitized excitation of 9-bromofluorene was achieved via 355-nm excitation of benzophenone. The triplet-triplet absorption spectrum of benzophenone is apparent at early times, for example 100 ps in Figure 8, and decays to give a spectrum (Figure 8, 19.5 ns) which is composed of absorptions due to the 9-fluorenyl radical and  $T_1$  of 9-bromofluorene. A comparison of Figures 7 and 8 at 19.5 ns shows that a weaker absorption due to the 9-fluorenyl radical relative to the triplet-triplet absorption of the 9-halofluorene results from 9-bromofluorene.

**Time-Resolved Fluorescence Measurements.** The time-dependence of the fluorescence resulting from 266-nm excitation of 0.15 mM fluorene in cyclohexane at 22 °C was measured. Fluorescence was detected for the wavelength range transmitted through a Corning 7-51 filter ( $> 10\%$  T for 320 nm  $< \lambda < 406$  nm with  $\% T_{\max} = 80\%$  at 365 nm). An observed fluorescence decay time ( $\tau_f$ ) of  $5.9 \pm 0.9$  ns was exhibited by this sample.

Our attempts to measure the fluorescence decay times of 2-bromofluorene, 9-chlorofluorene, and 9-bromofluorene have thus far been unsuccessful. The fluorescence intensities detected for these samples were too low at acceptable excitation pulse energies to permit reliable measurements of the short decay times. At high enough pulse energies to induce measurable time-dependent fluorescence, a stronger longer-lived fluorescence overwhelmed the weaker, shorter-lived fluorescence expected from the steady-state fluorescence spectroscopy of the 9-halofluorene.

## Discussion

**Absorption and Fluorescence Properties.** The absorption spectrum of fluorene in cyclohexane (Figure 1a) exhibits maxima at 300 ( $\epsilon \cong 10000$  M<sup>-1</sup> cm<sup>-1</sup>), 290 and 262 ( $\sim 20000$ ), and 220 nm ( $\sim 50000$ ). The maxima at 300 and 290 nm compose one system that is long-axis polarized as is the absorption band near 260 nm; the band near 220 nm is short-axis polarized as is a weak absorption system near 273 nm.<sup>32</sup> Substitution in the 2-position for 2-bromofluorene causes, as expected<sup>33</sup> and shown in Figure 1b, a bathochromic shift in the long-axis polarized absorptions of fluorene to 307 ( $\sim 10000$ ), 296, and 272 nm ( $\sim 30000$ ) with the strong, short-axis polarized band shifted to 206 nm ( $\sim 50000$ ). Substitution in the 9-position by chlorine (Figure 1c) leads to a decrease in intensity of the 300-nm system and the appearance of a new band near 235 nm ( $\sim 60000$ ) associated with transitions involving the halogen and probably short-axis polarized; the bands near 274 nm ( $\sim 30000$ ) and 210 nm ( $\sim 60000$ ) are not very much affected relative to 2-bromofluorene. For 9-bromofluorene (Figure 1d), all bands are less vibrationally structured and less intense. Maxima are exhibited near 279 ( $\sim 10000$ ), 242 ( $\sim 30000$ ), and 212 nm ( $\sim 30000$ ).

The fluorescence spectra of fluorene and 9-chlorofluorene are similar in appearance with two discernable maxima exhibited at 303 and 314 nm in Figure 1a and at 305 and 317 nm in Figure 1c, respectively. The fluorescence spectra of the 2-bromo- and 9-bromofluorene each exhibit a single maximum at 316 and 319 nm, respectively (Figures 1b and 1d).

The relative fluorescence quantum yields given above can be converted into absolute quantum yields with the use of a reported value of  $\phi_f$  for fluorene. A value of  $\phi_f = 0.80$  for fluorene in cyclohexane at 25 °C was reported by Berlmant<sup>24,25</sup> assuming the quantum yield of 9,10-diphenylanthracene to be 1.0. This assumption has been questioned.<sup>39</sup> Recent investigations have resulted in the report of an average value of 0.925 for  $\phi_f$  of 9,10-diphenylanthracene in cyclohexane.<sup>40,41</sup> This would lower  $\phi_f$  for fluorene from 0.80 to 0.74. More recently a value of  $\phi_f = 0.68$  was reported for 265-nm excitation of fluorene in degassed *n*-hexane at 293 K.<sup>23</sup> Using  $\phi_f = 0.68$  for fluorene, one obtains absolute fluorescence quantum yields of 0.024, 0.031, and 0.023 for 2-bromofluorene, 9-chlorofluorene, and 9-bromofluorene, respectively.

The fluorescence decay time of 5.8 ns observed for fluorene in our work compares well with the 5.1-ns decay time associated with the absorption assigned to  $S_n \leftarrow S_1$  transitions of fluorene in our transient absorption spectra. This agreement provides additional support for the assignment of the absorption in Figure 2 to the  $S_1$  state of fluorene. Our value of  $\tau_f$  does differ from several reported previously. The early, often quoted value of 10 ns was reported for a freeze-pump-thaw degassed cyclohexane solution at 25 °C.<sup>24,25</sup> In that experiment, the instrument response function had a full-width-at-half-maximum (fwhm) of

(34) Norman, I.; Porter, G. *Proc. R. Soc. London, Ser. A* **1955**, 230A, 399–414.

(35) Wong, P. C.; Griller, D.; Scaiano, J. C. *J. Am. Chem. Soc.* **1981**, 103, 5934–5935.

(36) Grasse, P. B.; Brauer, B.-E.; Zupancic, J. J.; Kaufmann, K. J.; Schuster, G. B. *J. Am. Chem. Soc.* **1983**, 105, 6833–6845.

(37) Trusov, V. V.; Teplyakov, P. A. *Opt. Spectrosc. (USSR)* **1964**, 16, 27–30.

(38) Kanda, Y.; Shimada, R.; Hanada, K.; Kajigaeshi, S. *Spectrochim. Acta* **1961**, 17, 1268–1274.

(39) Birks, J. B. *Photophysics of Aromatic Molecules*; Wiley-Interscience: New York, 1970.

(40) Meech, S. R.; Phillips, D. *J. Photochem.* **1983**, 23, 193–217.

(41) Maciejewski, A.; Steer, R. P. *J. Photochem.* **1986**, 35, 59–69.

3.4 ns.<sup>25</sup> In an experiment for which the instrument response function was 1.7 ns,<sup>42</sup> a  $\tau_f$  of 7.5 ns was reported for 265-nm excitation of a freeze-pump-thaw degassed *n*-hexane solution of fluorene at 293 K.<sup>23</sup> It is interesting to note that in this experiment,<sup>23</sup> the sum of  $\phi_f$  and the intersystem crossing quantum yield ( $\phi_i$ ) equals 0.93. For an air-equilibrated sample of fluorene in hexane, excitation with a nitrogen laser, presumably at 337 nm where fluorene exhibits an extremely low molar absorptivity, induced fluorescence which exhibited a decay time of  $3.8 \pm 0.1$  ns.<sup>27</sup> Time-correlated single-photon counting with an instrument response function of 2.8 ns fwhm yielded  $\tau_f = 3.36$  ns for an air-equilibrated, presumably room-temperature, cyclohexane solution of fluorene.<sup>26</sup> A consideration of the values of  $\tau_f$  for this variety of experimental conditions leads to the conclusion that our value of 5.8 ns for  $\tau_f$  is reasonable for our argon-bubbled sample of fluorene in which some oxygen is present.

**Possible Dissociation Modes.** Before beginning a discussion of our results in terms of mechanistic possibilities, a consideration of theoretically possible bond dissociation paths will be instructive. For the simpler case of photolysis of an alkyl halide, photodissociation of the C–X bond can occur from excited singlet and triplet states. The dissociation of a C–Cl or a C–Br bond can be considered to be a tetratomic<sup>43–45</sup> process involving the valence orbitals of the two atomic centers that separate as a result of bond rupture. These valence orbitals are the  $sp^3$  orbital of the carbon atom, the  $p$  orbital of the halogen used to form the  $\sigma$  bond to C, and the pair of  $p$  orbitals on the halogen atom that each contain a pair of nonbonding electrons. In a simplified consideration, the last pair of valence electrons on the halogen atom are assigned to the  $s$  orbital and are not considered further. The spin-orbital coupling in the relatively heavy atom, chlorine or bromine, removes the triple degeneracy of the atomic ground state, one of the dissociation products, to give a ground  $^2P_{3/2}$  state and an excited  $^2P_{1/2}$  state.

The states that correlate with the several dissociation limits of an alkyl halide are considered here. A ground-state alkyl radical is formed, plus a halogen atom in a ground ( $^2P_{3/2}$ ) or excited ( $^2P_{1/2}$ ) state is formed for each of the following: the nondegenerate singlet ground state  $S_0$  [ $^1A$ ] gives a ground-state X; the doubly degenerate singlet excited state  $S_1$  [ $^1E(n,\pi^*)$ ] gives excited-state X; the sextuply degenerate triplet excited state  $T_1$  [ $^3E(n,\pi^*)$ ] gives one-third excited-state X and two-thirds ground-state X; the triply degenerate triplet excited state  $T_2$  [ $^3A(\sigma,\sigma^*)$ ] gives ground-state X. The nondegenerate singlet excited state  $S_2$  [ $^1A(\sigma,\sigma^*)$ ] gives alkyl cation and halide ion. The incorporation of a  $\pi$  system, such as the fluorenyl moiety which is present in the arylmethyl halides studied in this work, introduces low-lying  $\pi,\pi^*$  states for geometries near vertical relative to the ground state equilibrium structure. These  $\pi,\pi^*$  states will intersect with the zero-order dissociative surfaces described above. For appropriate symmetries modified by vibronic coupling if necessary, these zero-order surfaces can mix at crossing points. Excited-state Cl has been detected in gas-phase photodissociations of chloroaromatic compounds.<sup>46,47</sup> In condensed phases, relaxation of the  $^2P_{1/2}$  excited state of Cl is expected to be very fast.

(42) Cehelnik, E. D.; Cundall, R. B.; Lockwood, J. R.; Palmer, T. F. *J. Phys. Chem.* **1975**, *79*, 1369–1376.

(43) Salem, L. *J. Am. Chem. Soc.* **1974**, *96*, 3486–3501.

(44) Dauben, W. G.; Salem, L.; Turro, N. J. *Acc. Chem. Res.* **1975**, *8*, 41–54.

(45) Michl, J.; Bonačić-Koutecký, V. *Electronic Aspects of Organic Photochemistry*; John Wiley & Sons, Inc.: New York, 1990.

(46) Tiemann, E.; Kanamori, H.; Hirota, E. *J. Chem. Phys.* **1988**, *88*, 2457–2468.

(47) Satyapal, S.; Tasaki, S.; Bersohn, R. *Chem. Phys. Lett.* **1993**, *203*, 349–352.

**Dissociation Modes Consistent with Our Experimental Data.** Although no  $S_n \leftarrow S_1$  absorptions are detectable at early times for direct excitation of 9-chlorofluorene and 9-bromofluorene in cyclohexane, the recorded fluorescence spectra indicate a lifetime for  $S_1$  prior to bond dissociation and population of  $T_1$ . The  $S_n \leftarrow S_1$  absorptions must be too weak because of their short lifetimes and molar absorptivities to allow their detection with our laser system.

For 9-chlorofluorene,  $T_n \leftarrow T_1$  absorptions and the 9-fluorenyl radical appear with time constants of  $\sim 40$  ps and persist for  $> 20$  ns. For 9-bromofluorene,  $T_n \leftarrow T_1$  absorptions and the 9-fluorenyl radical appear with time constants of  $\leq 20$  ps and persist for  $> 20$  ns. These observations are consistent with homolytic dissociation from an excited singlet state which is also depleted *via* intersystem crossing on a time scale of tens of picoseconds to give a triplet state which is nondissociative in this time regime. Another possibility which cannot be rigorously excluded at this time, but seems unlikely, is the population of an upper triplet state which rapidly competitively undergoes dissociation and relaxation to  $T_1$  which is nondissociative in this time regime.

Intersystem crossing leading to the population of  $T_1$  occurs rapidly enough to compete with the very fast bond homolysis in the 9-halofluorenes. Although the halogen in 9-chloro- or 9-bromofluorene is not directly attached to the  $\pi$  system as is the case for 2-bromofluorene, the 9-halo substituent is very effective in enhancing SOC and increasing the rate of intersystem crossing relative to fluorene. Effects of intramolecular “external” heavy atoms have been reported<sup>48</sup> for a series of bromobenzonorbornenes and bromonaphthonorbornenes. However, the effects of the bromine substituent on the electronic absorption spectra of the parent arenonorbornenes were not described, so a comparison with the spectra of the fluorenes studied in our work cannot be made here.

Triplet sensitization leads to the production of the 9-fluorenyl radical from 9-chlorofluorene and 9-bromofluorene with less formed from 9-bromofluorene. The yields of radical are very small relative to the yields of  $T_1$ . Because the energies of  $T_1$  and  $T_2$  of 9-chloro- and 9-bromofluorene are not known, the possibility of populating  $T_2$  *via* benzophenone sensitization is not known with certainty but may be expected to be unlikely because of the relative energies of  $T_1$  of benzophenone and fluorene. The involvement of  $T_2$  has been proposed, for example, in photosolvolysis studies of benzyl chloride.<sup>17</sup> Another, perhaps more likely, possibility for benzophenone sensitization of the 9-halofluorenes is that the low yields of radicals result from the involvement of a triplet exciplex as was proposed for a similar observation made in studies of 1-(chloromethyl)naphthalene.<sup>14</sup> The greater amount of radical from the chloride than from the bromide in the sensitized experiments may reflect the observed greater propensity of the chloride to give radical in the direct photolysis.

## Conclusions

For photodissociations of carbon-heteroatom (C–X) bonds in molecules in solution, questions which need to be addressed include the following:

- (1) How long does the molecule reside within the excited singlet state manifold?
- (2) How rapidly does the excited singlet molecule undergo intersystem crossing to the triplet manifold?
- (3) Does the C–X bond undergo dissociation in the singlet and/or the triplet manifold?

(48) Chandra, A. K.; Turro, N. J.; Lyons, A. L. J.; Stone, P. *J. Am. Chem. Soc.* **1978**, *100*, 4964–4968.

(4) Does the C–X bond cleavage occur homolytically or heterolytically?

(5) Do the pairs of fragments resulting from bond heterolysis and homolysis interconvert *via* electron transfer?

In this work, we have focused on questions 1–4 for photoinduced bond homolysis in 9-chlorofluorene and 9-bromofluorene. Our results can be considered in terms of Scheme 1. It has been learned that intersystem crossing from  $S_1$  to  $T_1$  in 2-bromofluorene occurs efficiently with a time constant of  $\sim 40$  ps ( $k_{isc} \cong 2.5 \times 10^{10} \text{ s}^{-1}$ ). Intersystem crossing from  $S_1$  to  $T_1$  occurs with time constants of  $\sim 40$  ps ( $k_{isc} \cong 2.5 \times 10^{10} \text{ s}^{-1}$ ) and  $\leq 20$  ps ( $k_{isc} \geq 5.0 \times 10^{10} \text{ s}^{-1}$ ) for 9-chlorofluorene and 9-bromofluorene, respectively; the appearance of the ground-state 9-fluorenyl radical occurs with time constants of  $\sim 40$  ps ( $k_{hom} \cong 2.5 \times 10^{10} \text{ s}^{-1}$ ) and  $\leq 20$  ps ( $k_{hom} \geq 5.0 \times 10^{10} \text{ s}^{-1}$ ) for 9-chlorofluorene and 9-bromofluorene, respectively. There is no evidence of geminate recombination in our transient absorption spectra.

Our currently preferred explanation for the difference between the relative amounts of 9-fluorenyl radical produced from direct excitation of 9-chlorofluorene *vs* 9-bromofluorene is that bond homolysis occurs in the singlet manifold which is depleted *via* intersystem crossing to the triplet manifold and the population of  $T_1$  which does not undergo dissociation ( $k_{hom}$ ) in the  $< 20$ -ns time regime. The rate of intersystem crossing is faster for 9-bromofluorene so the time spent in the singlet manifold, where bond homolysis is occurring, is less; this results in less production of the 9-fluorenyl radical although the C–Br bond is weaker than the C–Cl bond. An alternative path, which cannot be rigorously excluded at this time but which may be considered less likely, is one involving the population of an upper dissociative triplet state prior to relaxation to the nondissociative  $T_1$  state. Experiments to test mechanistic alternatives are planned.

## Experimental Section

**Materials.** Fluorene (Aldrich, 98%) was recrystallized twice from ethanol. Note that fluorene in this work refers to 9*H*-fluorene. 2-Bromofluorene (Aldrich, 98%) was recrystallized from hexane. 9-Bromofluorene (Aldrich, 95%) was recrystallized twice from cyclohexane. 9-Chlorofluorene<sup>49</sup> was synthesized by the reaction of 9-fluorenol with concentrated hydrochloric acid and was recrystallized twice from hexane. 9-Fluorenol<sup>50–52</sup> was prepared by the reduction of 9-fluorenone (Aldrich, 98%, recrystallized from ethanol) with lithium aluminum hydride (Aldrich, 95+%). Benzophenone (Fisher, certified) was purified by sublimation. Cyclohexane (Fisher, HPLC grade) was used as received.

**Steady-State Spectroscopy.** Electronic absorption spectra were recorded on a Shimadzu UV-2100 UV–vis spectrophotometer. Optical cells that were used had path lengths of 2 mm and 1 cm.

Fluorescence spectra were recorded on a Perkin-Elmer Hitachi MPF-2A spectrophotometer. Samples with concentrations ranging from 2.0 to 8.0  $\mu\text{M}$  in cyclohexane were bubbled with argon for 10 to 20 min and placed in Teflon-stoppered 1-cm fluorescence cells. Fluorescence spectra were corrected for variations in instrument response as a function of wavelength.

**Picosecond Laser Spectroscopy.** The modified Quantel/Continuum Nd:YAG laser system used to record the transient absorption spectra and time-dependent fluorescence data has been described previously.<sup>53</sup> Briefly, it consists of an actively–passively mode-locked Nd:YAG oscillator and a double-pass Nd:YAG amplifier. Excitation pulses exhibiting a half width of  $\sim 25$  ps at 266 and 355 nm were generated

from the 1064-nm fundamental by means of harmonic-generating crystals. The energies of the excitation pulses were measured by diverting  $\sim 10\%$  of each pulse into the probe (Model RJP-735) of an energy meter (Laser Precision Corp. Model RJ-7200) and were in the range of 0.14–0.22 mJ/pulse. The energies of the excitation laser pulses were in the range for which the signal intensity depended linearly on pulse energy. The beam diameter at the sample was  $\sim 2$  mm.

Transient absorption spectra were recorded at selected times after excitation at 22 °C. The absorbance change as a function of wavelength was monitored by means of an  $\sim 30$ -ps continuum pulse. This white-light probe pulse was generated when the sufficiently energetic portion of the split, original 1064-nm pulse was focused into a 20-cm cell that contained a  $\text{D}_2\text{O}/\text{H}_2\text{O}$  mixture. The probe pulse was split, directed through the sample cell and the reference cell, and focused at the slit of a 0.32-m spectrograph (Instruments SA Model HR-320). The spectrograph output was imaged onto an EG&G Princeton Applied Research (PAR) two-dimensional silicon intensified target (SIT) detector (Model 1254E) coupled to a PAR 1216 multichannel detector controller. This detector was interfaced with an IBM microcomputer that controlled the necessary optical hardware and electronics during data acquisition, processed the data, and presented the data graphically. To improve the signal-to-noise ratio, each difference absorption spectrum is the result of averaging data from at least 400 excitation laser pulses. A difference absorption spectrum spanning a wavelength range from  $\sim 430$  to 790 nm is the result of splicing two spectra recorded in the 430–640-nm and the 560–790-nm regions at a selected time after excitation. To acquire data for each transient absorption spectrum, the sample was flowed through a 2-mm or 5-mm path length fused silica flow cell at a rate sufficient to replace the volume that was exposed to the excitation pulses impinging on the sample at a rate of 10 pulses/s. The samples used for the transient absorption experiments on fluorene and 2-bromofluorene were argon-bubbled for 10 to 20 min and maintained under a positive pressure of argon during an experiment. The sample solutions for the transient absorption data involving direct excitation of 9-chlorofluorene and 9-bromofluorene and all triplet excitation transfer experiments were bubbled with a stream of argon for 45 to 60 min prior to an experiment and maintained under a positive pressure of argon during an experiment. The reported time constants for the decay of  $S_n \leftarrow S_1$  absorptions of fluorene and 2-bromofluorene, which have uncertainties of  $\pm 15\%$ , are the results of least-squares best fits of the experimental data in which the instrument response function is taken into account. The rise times given for the appearance of the triplet–triplet absorptions of 2-bromofluorene, 9-chlorofluorene, and 9-bromofluorene and for the appearance of the 9-fluorenyl radical following excitation of 9-chlorofluorene and 9-bromofluorene are estimates resulting from comparisons of the experimental data with calculated kinetic curves which take into account the instrument response function.

Time-dependent fluorescence data were measured at 22 °C, as described previously,<sup>53</sup> with the use of the ps-pulsed Nd:YAG laser system and a Hamamatsu C979-01 temporal disperser coupled to a PAR 1254 SIT detector whose output is digitized with a PAR 1216 multichannel detector controller interfaced with a microcomputer. Samples were argon-bubbled for 45 to 60 min prior to an experiment and maintained under a positive pressure of argon during an experiment. Long-wave pass or bandpass filters were used to isolate the spectral regions of interest. The reported observed decay times, which have uncertainties of  $\pm 15\%$ , are the results of least-squares best fits of the experimental data with the instrument response function taken into account.

UV absorption spectra of the samples were recorded before and after the laser experiments to ensure that the samples had not undergone significant irreversible photochemical changes during the course of the time-resolved measurements.

**Acknowledgment.** Financial support from the National Science Foundation is gratefully acknowledged.

JA944100E

(49) Hurd, C. D.; Mold, J. D. *J. Org. Chem.* **1948**, *13*, 339–345.

(50) Friedrich, E. C.; Taggart, D. B. *J. Org. Chem.* **1978**, *43*, 805–808.

(51) Hochstein, F. A. *J. Am. Chem. Soc.* **1949**, *71*, 305–307.

(52) Brown, W. G. *Org. React.* **1951**, *6*, 469–509.

(53) Schmidt, J. A.; Hilinski, E. F. *Rev. Sci. Instrum.* **1989**, *60*, 2902–2914.